



ChemComm

**Hydrogen Bonding between Hydroxylic Donors and MLCT-
Excited $\text{Ru}(\text{bpy})_2(\text{bpz})^{2+}$ Complex: Implications for
Photoinduced Electron-Proton Transfer**

Journal:	<i>ChemComm</i>
Manuscript ID	CC-COM-03-2019-001896.R1
Article Type:	Communication

SCHOLARONE™
Manuscripts

COMMUNICATION

Hydrogen Bonding between Hydroxylic Donors and MLCT-Excited $\text{Ru}(\text{bpy})_2(\text{bpz})^{2+}$ Complex: Implications for Photoinduced Electron-Proton Transfer

Received 00th January 20xx,
Accepted 00th January 20xx

Sergei V. Lymar,^{a*} Gerald F. Manbeck,^a and Dmitry E. Polyansky^{a*}

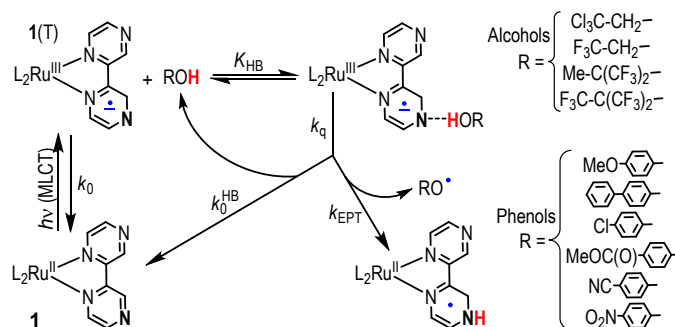
DOI: 10.1039/x0xx00000x

The equilibrium constants of hydrogen bonding (HB) between hydroxylic donors, ROH, and MLCT-excited $\text{Ru}(\text{bpy})_2(\text{bpz})^{2+}$ complex, $\mathbf{1}(\text{T})$ correlate with ROH empirical HB acidities, which is used for evaluating the unimolecular rate constants of concerted electron-proton transfer within the H-bonded Phenol- $\mathbf{1}(\text{T})$ exciplexes.

Formation of a precursor complex with hydrogen bonded (HB) proton donor and acceptor reactant moieties is a prerequisite for concerted electron-proton transfer (EPT).¹⁻⁶ As a result, kinetic expressions for experimentally determinable rate of EPT reactions invariably contain a product of the H-bonding equilibrium constant, K_{HB} , and the unimolecular rate constant for the EPT step, k_{EPT} , which are often difficult or impossible to separate and evaluate individually. These difficulties are particularly severe for rapid photoinduced EPT reactions,⁷⁻¹² such as EPT from phenolic donors to a polypyridine Ru complex with a proton-accepting ligand ($\mathbf{1} = \text{Ru}(\text{bpy})_2(\text{bpz})^{2+}$, where bpy = 2,2'-bipyridine and bpz = 2,2'-bipyrazine) (Scheme 1).^{13, 14} In this system, photoexcitation of $\mathbf{1}$ followed by rapid intersystem crossing yields the triplet metal-to-ligand charge transfer (MLCT) state, $\mathbf{1}(\text{T})$. The now formal Ru^{III} center becomes an electron acceptor while the Brønsted basicity of the uncoordinated N atoms in bpz ligand is increased, creating a driving force for excited state quenching of $\mathbf{1}(\text{T})$ through EPT from electron-proton donors. Additionally, excess electron on bpz increases K_{HB} with electron-proton donors and HB donors in general. In addition to bringing $\mathbf{1}(\text{T})$ and a donor in close proximity and proper alignment for EPT, this H-bonding may modulate the triplet state lifetime through a physical quenching mechanism that competes with EPT. In the context of Scheme

$\mathbf{1}$, the term "physical quenching" encompasses all processes that lead to deactivation of the ROH- $\mathbf{1}(\text{T})$ exciplex without creating separated electron transfer, proton transfer or EPT products. In a more narrow sense, this term was used by Linschitz and co-workers for acceleration of radiationless transition in H-bonded pairs.¹⁵

Scheme 1. General mechanism of a photoinduced reactivity of $\text{Ru}(\text{bpy})_2(\text{bpz})^{2+}$ complex toward a hydroxylic ROH compound invoking their H-bonding preequilibrium. Shown on the right is the set of ROH compounds used in this work.



In terms of Scheme 1, the Stern-Volmer expression for the observed triplet emission intensity (I_{obs}) and decay lifetime (τ_{obs}) in the presence of a hydroxylic quencher (ROH) is given by^{13, 14}

$$\frac{I_0}{I_{\text{obs}}} = \frac{\tau_0}{\tau_{\text{obs}}} = 1 + \frac{\tau_0(k_q - k_0)K_{\text{HB}}[\text{ROH}]}{1 + K_{\text{HB}}[\text{ROH}]} = 1 + \frac{\tau_0 k_q^{\text{obs}}[\text{ROH}]}{1 + K_{\text{HB}}[\text{ROH}]} \quad (1)$$

where I_0 and $\tau_0 = 1/k_0$ are the corresponding intensity and lifetime of $\mathbf{1}(\text{T})$ emission in the absence of quencher, $[\text{ROH}]$ is the concentration of added quencher, K_{HB} is the equilibrium constant for H-bonding between $\mathbf{1}(\text{T})$ and ROH, and $k_q = k_q^{\text{HB}} + k_{\text{EPT}}$ is a combined first-order rate constant for the physical quenching and EPT reaction. The values of τ_0 , K_{HB} , and k_q are generally solvent-dependent. It is clear from eq. 1 that the determination of both k_q and K_{HB} requires data in the range where $K_{\text{HB}}[\text{ROH}] \gg 1$, and the Stern-Volmer dependence approaches a plateau. However, in all studies of EPT from phenolic donors in systems analogous to that in Scheme 1 these

^a Chemistry Division, Brookhaven National Laboratory, Upton, New York 11973-5000, U.S.A.

†Electronic Supplementary Information (ESI) available: materials and methods, Stern-Volmer lifetime plots for quenching of $\mathbf{1}(\text{T})$ in CH_2Cl_2 , dependence of $\log k_q$ on α_2^{H} , transient absorption spectra of $\mathbf{1}(\text{T})$, van't Hoff plots for the HB between $\mathbf{1}(\text{T})$ and alcohols, the dependence of the enthalpy and entropy for the HB between $\mathbf{1}(\text{T})$ and halogenated alcohols on α_2^{H} . See DOI: 10.1039/x0xx00000x

plateaus could not be reached⁷⁻¹² due to a combination of two factors: (i) low K_{HB} values along with insufficient ROH solubility, and (ii) high quenching efficiencies (k_{q} values) that made both I_{obs} and τ_{obs} immeasurably small at relatively low [ROH], well before the $K_{\text{HB}}[\text{ROH}] \gg 1$ condition is satisfied. As a result, Stern-Volmer plots showed only small, if any, downward curvature, and only the bimolecular rate constants $k_{\text{q}}^{\text{obs}} = (k_{\text{q}} - k_0)K_{\text{HB}}$ could be measured reliably.

Recently, we have used 2,2,2-trifluoroethanol ($\text{CF}_3\text{CH}_2\text{OH}$) as a surrogate for *p*-methoxyphenol (*p*-MeOPhOH) with respect to H-bonding with **1**(T) and analogous complexes in dichloromethane.¹³ This approach is predicated on the similarity of the H-bond donating capacities of $\text{CF}_3\text{CH}_2\text{OH}$ and *p*-MeOPhOH on the Abraham α_2^{H} scale devised for evaluating the molar-based formation equilibrium constants (K_{AHB}) of 1:1 complexes between uncharged H-bond donors (AH) and acceptors (B) in CCl_4 ; that is,

$$\log K_{\text{AHB}} = 7.354\beta_2^{\text{H}}(\text{B})\alpha_2^{\text{H}}(\text{AH}) - 1.094 \quad (2)$$

where the empirically-defined parameters $0 < \alpha_2^{\text{H}}(\text{AH}) < 1$ and $0 < \beta_2^{\text{H}}(\text{B}) < 1$ are termed HB acidity and basicity, respectively.¹⁶ Accessing K_{HB} for the $\text{CF}_3\text{CH}_2\text{OH}$ -**1**(T) exciplex is made possible by both the high solubility and low quenching efficiency of the alcohol; the latter is due to high $\text{CF}_3\text{CH}_2\text{O-H}$ bond dissociation free energy and attendant absence of the EPT pathway. In this communication, we further explore this approach by investigating H-bonding equilibria in CH_2Cl_2 between **1**(T) and a series of hydroxylic HB acids that includes halogenated aliphatic alcohols and *p*-substituted phenols with α_2^{H} in the 0.5-0.9 range (Scheme 1).

Under the pseudo-first-order conditions with a large excess of ROH over **1**(T), all observed **1**(T) emission decays were fit to single exponential kinetics, from which the τ_{obs} values were determined (see ESI for experimental details). Due to solubility limitations and/or high quenching efficiencies, Stern-Volmer quenching plots exhibiting well-defined saturation were obtained only for the alcohols, *p*-cyanophenol, and *p*-nitrophenol. The K_{HB} and k_{q} values derived from these plots using eq. 1 are summarized in Table 1. For other, less acidic phenols in Scheme 1, Stern-Volmer quenching plots were linear in the entire experimentally accessible ROH concentration range, and only the effective bimolecular rate constants $k_{\text{q}}^{\text{obs}} = (k_{\text{q}} - k_0)K_{\text{HB}}$ could be evaluated using eq. 1.¹³ These $k_{\text{q}}^{\text{obs}}$ values are listed in Table 2.

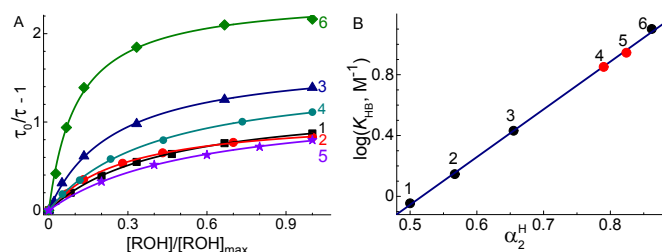


Fig. 1. (A) Stern-Volmer plots for quenching of **1**(T) by alcohols and phenols in CH_2Cl_2 at 25 °C, where $\tau_0 = 585$ ns. The concentration axis is normalized to the highest concentration for each quencher ($[\text{ROH}]_{\text{max}}$; for details, see Fig. S1, ESI). (B) Dependence of $\log K_{\text{HB}}$ upon HB acidity of alcohols (1-3, and 6) and phenols (4 and 5) with the linear

fit, whose slope and intercept are 3.14 ± 0.05 and -1.63 ± 0.03 , respectively. The numerical labels correspond to entries in Table 1.

The k_{q} values in Table 1 indicate that the triplet lifetimes of ROH-**1**(T) exciplexes (170-260 ns) are 2.3-3.4 times shorter than the lifetime of free **1**(T) in the same solvent. This observation is in line with literature reports on the lifetime shortening of the excited states of organic compounds and coordination complexes facilitated by exciplex formation.¹⁷⁻¹⁹ A good linear correlation between $\log k_{\text{q}}$ and α_2^{H} (Fig. S2, ESI) suggests the same principal mechanism for accelerating decay of **1**(T) by its H-bonding to all alcohols in Table 1. Because EPT from alcohols is expected to be thermodynamically unfavorable due to high BDE of their RO-H bonds,^{13, 20, 21} this mechanism must primarily involve the physical quenching route in Scheme 1; i.e., $k_{\text{q}} = k_0^{\text{HB}} + k_{\text{EPT}}$ is dominated by the k_0^{HB} term. This assertion is supported by the transient absorption data (Fig. S3, ESI) showing complete absence of photoproducts associated with quenching of **1**(T) by two alcohols, $\text{CCl}_3\text{CH}_2\text{OH}$ and $(\text{CF}_3)_3\text{COH}$, occupying low and high ends of the α_2^{H} range.

While the physical quenching mechanism is not yet clear, we consider two factors involved in accelerating the excited state triplet to the ground state singlet via radiationless transition in the ROH-**1**(T) exciplexes, namely, the increase of the spin-orbit coupling and facilitating triplet energy dissipation due to the triplet-singlet vibronic coupling through the readily dissociable H-bond.¹⁵

Notably, the $\log k_{\text{q}}$ values for *p*-nitro- and *p*-cyanophenol lie sufficiently close to the alcohol line in Fig. S2, ESI, which suggests the prevalence of the same physical quenching mechanism. In the absence of this evidence, it would be easy to mistakenly ascribe quenching by these phenols to the occurrence of slow EPT reactions.

Table 1. Equilibrium constants, enthalpies, and entropies (K_{HB} , ΔH_{HB} , and ΔS_{HB}) for H-bonding of hydroxylic HB acids (ROH) to **1**(T) and unimolecular rate constants (k_{q}) of emission decay for the ROH-**1**(T) exciplexes in CH_2Cl_2 at 25 °C.^a

No	R-	α_2^{H} , ^b	k_{q} , ^c 10^6 s^{-1}	K_{HB} , ^c M^{-1}	$-\Delta H_{\text{HB}}$, ^d kcal/mol	$-\Delta S_{\text{HB}}$, ^d cal/(mol K)
1	CCl_3CH_2-	0.500	3.9	0.9	4.1	14
2	CF_3CH_2-	0.567	3.6	1.4	4.2	13
3	$\text{MeC}(\text{CF}_3)_2-$	0.655	4.7	2.7	4.3	13
4	$\text{NC}-\text{C}_6\text{H}_4-$	0.790	4.4	7.1	n/d ^e	n/d ^e
5	$\text{O}_2\text{N}-\text{C}_6\text{H}_4-$	0.824	3.8	8.9	n/d ^e	n/d ^e
6	$\text{CF}_3\text{C}(\text{CF}_3)_2-$	0.862	5.8	12.6	4.8	10

^aFor data uncertainties, see Table S1, ESI; ^bFrom ref.22; ^cObtained from fitting Stern-Volmer plots in Fig. S1, ESI to eq. 1; ^dObtained from K_{HB} temperature dependencies in Fig. S4, ESI; ^eNot determined.

The H-bonding enthalpies and entropies obtained from the van't Hoff plots for K_{HB} over the -20 to $+40$ °C temperature range (Fig. S4, ESI) and included in Table 1 are all negative as expected, and their magnitudes are consistent with H-bonding. Although relatively small, the changes in ΔH_{HB} , and ΔS_{HB} are systematic (Fig. S5, ESI). While the H-bond strength increases with the ROH acidity, the ΔS_{HB} values become less negative, and

both these trends contribute to the K_{HB} increase with α_2^{H} (Table 1 and Fig. 1).

In fact, there is a very good linear correlation between the HB acidities of ROH and free energies of their H-bonding to **1(T)** shown in Fig. 1B; that is,

$$\log K_{\text{HB}} = -\Delta G_{\text{HB}}/2.30RT = 3.14\alpha_2^{\text{H}} - 1.63 \quad (3)$$

This correlation validates our conjecture that the α_2^{H} parameter developed to describe H-bonding to neutral HB acceptors can also serve as a thermodynamic descriptor for the H-bonding to charged, dipolar acceptors, such as complex **1(T)**.

Moreover, the value of eq. 3 is emphasized for evaluating K_{HB} and deriving $k_{\text{q}} = k_0 + k_{\text{q}}^{\text{obs}}/K_{\text{HB}}$ for less HB-acidic but more strongly quenching phenols for which these quantities could not be measured directly (Table 2). It can be seen that all k_{q} values for these phenols are greater than k_{q} for any ROH in Table 1 and sharply increase with decreasing phenol's O-H bond dissociation free energy (BDFE). This behavior is attributable to the growing contribution from the EPT pathway to the overall decay of ROH-**1(T)** exciplex (Scheme 1), which, as we have shown in the previous studies,^{13, 14} arises from the more favorable EPT driving force for phenols with smaller O-H BDFE.

Table 2. Observed bimolecular rate constants ($k_{\text{q}}^{\text{obs}}$), H-bonding equilibrium constants (K_{HB}), and unimolecular rate constants (k_{q} and k_0^{HB}) for reaction of *p*-substituted phenols with **1(T)** in CH_2Cl_2 at 25 °C. Also shown are BDFE of phenols' O-H bonds.^a

Phenol	α_2^{H} ^b	K_{HB} , ^c M ⁻¹	$k_{\text{q}}^{\text{obs}}$, ^d 10 ⁷ M ⁻¹ s ⁻¹	k_{q} , ^e 10 ⁶ s ⁻¹	k_0^{HB} , ^f 10 ⁶ s ⁻¹	BDFE, ^g kcal/mol
MeO-C ₆ H ₄ -OH	0.573	1.5	150	1000	3.5	79.6
Ph-C ₆ H ₄ -OH	0.595	1.7	42	240	3.6	82.1
Cl-C ₆ H ₄ -OH	0.670	3.0	6.0	22	4.0	86.1
MeOC(O)-C ₆ H ₄ -OH	0.730	4.6	2.0	6.1	4.3	88.4

^aFor data uncertainties, see Table S2, ESI; ^bFrom ref. 22, except for MeOC(O)-phenol, which is from ref. 13; ^cEvaluated using eq. 3; ^dIn CH_2Cl_2 , from ref. 13; ^eCalculated using eq. 1; ^fEstimated from data in Fig. S2, ESI; ^gIn CH_2Cl_2 , from ref. 13, ± 2 kcal/mol.

Shown in Fig. 2 is a correlation of the rate constants for the overall quenching and EPT pathway with the EPT thermodynamic driving force that linearly decreases with the increase of phenol's O-H BDFE. The k_{EPT} values for this plot have been obtained by correcting the overall quenching rate constant for the contribution of physical quenching, that is, $k_{\text{EPT}} = k_{\text{q}} - k_0^{\text{HB}}$. For *p*-Ph- and *p*-MeO-phenol, these corrections are negligible, but for *p*-Cl- and, especially, for *p*-MeOC(O)-phenol, the values of k_{q} and k_0^{HB} are comparable. Thus, the data in Table 2 and Fig. 2 clearly show that the contribution of physical quenching to measured k_{q} can be significant, particularly in the low driving force regime. These findings forewarn of a pitfall associated with a common practice^{2, 23, 24} of attributing the overall rate of the excited state quenching entirely to EPT or other chemical process, when an H-bonding pre-equilibrium may be involved.

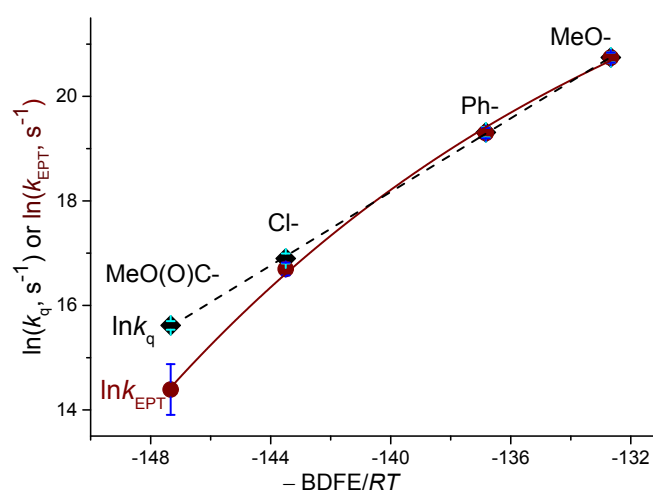


Fig. 2. Rate-free energy correlation for the reaction between **1(T)** and four *p*-substituted phenols from Table 2. The BDFE values have been multiplied by -1 to show increasing EPT driving force along the horizontal axis. No theoretical significance is assigned to the lines, which are shown as the visual aids only. The error bars are obtained from propagating experimental uncertainties.

In summary, our work demonstrates that: (1) hydroxylic HB donors (halogenated alcohols or *p*-substituted phenols) form H-bonded exciplexes with an MLCT excited polypyridine Ru complex containing a proton-accepting ligand, (2) halogenated alcohols can be used to obtain H-bonding equilibrium constants together with rate constants for physical quenching in these exciplexes, (3) a linear correlation exists between the free energy of H-bonding and the HB acidities of hydroxylic donors. This correlation allows an accurate prediction of HB equilibrium constants in systems where they cannot be measured directly, and (4) the decay of an H-bonded exciplex always involves a physical quenching pathway concurrent with the electron-proton transfer. Depending upon the EPT driving force (ΔG_{EPT}), the contribution of this pathway to the observed overall quenching varies from insignificant for high ΔG_{EPT} , to dominant at low driving forces.

This work was carried out at Brookhaven National Laboratory and supported by the U.S. Department of Energy, Office of Science, Office of Basic Energy Sciences, Division of Chemical Sciences, Geosciences, & Biosciences, under contract DE-SC0012704.

Conflicts of interest

There are no conflicts to declare.

Notes and references

- P. Dongare, A. G. Bonn, S. Maji and L. Hammarström, *J. Phys. Chem. C*, 2017, **121**, 12569-12576.
- L. Biczok and H. Linschitz, *J. Phys. Chem.*, 1995, **99**, 1843-1845.
- D. R. Weinberg, C. J. Gagliardi, J. F. Hull, C. F. Murphy, C. A. Kent, B. C. Westlake, A. Paul, D. H. Ess, D. G. McCafferty and T. J. Meyer, *Chem. Rev.*, 2012, **112**, 4016-4093.

4. J. M. Saveant and C. Tard, *J. Am. Chem. Soc.*, 2014, **136**, 8907-8910.
5. L. A. Clare, A. T. Pham, F. Magdaleno, J. Acosta, J. E. Woods, A. L. Cooksy and D. K. Smith, *J. Am. Chem. Soc.*, 2013, **135**, 18930-18941.
6. J. M. Mayer, *Annu. Rev. Phys. Chem.*, 2004, **55**, 363-390.
7. C. Bronner and O. S. Wenger, *J. Phys. Chem. Lett.*, 2012, **3**, 70-74.
8. J. J. Concepcion, M. K. Brennaman, J. R. Deyton, N. V. Lebedeva, M. D. E. Forbes, J. M. Papanikolas and T. J. Meyer, *J. Am. Chem. Soc.*, 2007, **129**, 6968-6969.
9. A. A. Pizano, J. L. Yang and D. G. Nocera, *Chem. Sci.*, 2012, **3**, 2457-2461.
10. J. Chen, M. Kuss-Petermann and O. S. Wenger, *Chem. Eur. J.*, 2014, **20**, 4098-4104.
11. M. Kuss-Petermann and O. S. Wenger, *J. Phys. Chem. A*, 2013, **117**, 5726-5733.
12. N. V. Lebedeva, R. D. Schmidt, J. J. Concepcion, M. K. Brennaman, I. N. Stanton, M. J. Therien, T. J. Meyer and M. D. E. Forbes, *J. Phys. Chem. A*, 2011, **115**, 3346-3356.
13. S. V. Lymar, M. Z. Ertem and D. E. Polyansky, *Dalton Trans.*, 2018, **47**, 15917-15928.
14. S. V. Lymar, M. Z. Ertem, A. Lewandowska-Andralojc and D. E. Polyansky, *J. Phys. Chem. Lett.*, 2017, **8**, 4043-4048.
15. L. Biczók, T. Bérces and H. Linschitz, *J. Am. Chem. Soc.*, 1997, **119**, 11071-11077.
16. M. H. Abraham, *Chem. Soc. Rev.*, 1993, **22**, 73-83.
17. D. K. C. Tears and D. R. McMillin, *Coord. Chem. Rev.*, 2001, **211**, 195-205.
18. U. Pischel and W. M. Nau, *J. Am. Chem. Soc.*, 2001, **123**, 9727-9737.
19. O. Horvath, *Coord. Chem. Rev.*, 1994, **135**, 303-324.
20. Y.-R. Luo, *Comprehensive Handbook of Chemical Bond Energies*, CRC Press, Boca Raton, 2007.
21. K. U. Ingold and J. S. Wright, *J. Chem. Educ.*, 2000, **77**, 1062-1064.
22. M. H. Abraham, P. P. Duce, J. J. Morris and P. J. Taylor, *J. Chem. Soc., Faraday Trans. 1*, 1987, **83**, 2867-2881.
23. M. Kuss-Petermann and O. S. Wenger, *J. Phys. Chem. Lett.*, 2013, **4**, 2535-2539.
24. J. Nomrowski and O. S. Wenger, *Inorg. Chem.*, 2015, **54**, 3680-3687.